4-2011

The Immunophenotypic and Cytokine Characterization of the Osteoarthritic Human Patellar Fat Pad: Comparison to Subcutaneous Adipose Tissue

Katie Marie Hamel

The Immunophenotypic and Cytokine Characterization of the Osteoarthritic Human Patellar Fat Pad: Comparison to Subcutaneous Adipose Tissue

by

Katie Marie Hamel

Undergraduate honors thesis under the direction of

Dr. Jeffrey M. Gimble

Department of Stem Cell Biology, Pennington Biomedical Research Center

Submitted to the LSU Honors College in partial fulfillment
of the Upper Division Honors Program

April 2011

Louisiana State University
& Agricultural and Mechanical College
Baton Rouge, Louisiana

Acknowledgments

First, I would like to thank Dr. Jeffrey M. Gimble for giving me the opportunity to be a part of the Stem Cell Biology Laboratory at Pennington Biomedical Research. As a mentor, he has provided me with indispensable advice and opened the doors to a wave of opportunities. His vast knowledge and passion for the field has profoundly impacted my interest in research and desire to continue research while pursuing a medical degree. Most importantly, his confidence in me as both an individual and student made the completion of this research study possible.

I would like to thank all of those who dedicated their time and effort throughout the duration of the study. This achievement would not have been possible without the collaboration of several groups including: Dr. Dasa, Dr. Duarte, Dr. Zhang, and Constance Porretta of LSU Health Sciences Center; Masudul Haque, Dr. Lopez, and Marilyn Dietrich of LSU Veterinary Medicine; and especially all of the members of the Stem Cell Biology Lab at Pennington Biomedical Research Center including Xiying Wu and Forum Shah.

I would also like to thank Dr. James W. Wade and his practice for providing lipoaspirate samples for this study.

A special thanks to Pedro Pires de Carvalho, whose help, guidance, and dedication to the study was indispensable and greatly appreciated.

I would like to especially thank my parents for giving me the opportunity to pursue my dreams. For the past twenty-three years, they have devoted every ounce of themselves to ensure that I have every opportunity to succeed. They have provided me with all of the tools I need to achieve my goals. I owe all of my achievements as a student and as an athlete to my parents.

Each member of my family deserves a special thanks for believing in me and providing unwavering support every step of the way.

This project was funded by LSU Health Sciences Center Department of Orthopaedics and Medicine as well as the Pennington Biomedical Research Foundation.

Table of Contents

List of Tables

List of Figures

Abstract

Adipose tissue plays an integral role in the human body. Current research has indicated that in addition to energy storage and release, adipose tissue behaves as an endocrine organ. Both the secretion of adipokines such as adiponectin and leptin and the presence of adipose-bound receptors enhance the communication between adipose tissue and other organs including the central nervous system. The interaction between adipose tissue and the central nervous system affects several biological processes including metabolism, neuroendocrine function, and immune response. Adipose tissue is not only composed of adipocytes, but it also houses several other cell types including endothelial, immune, and mesenchymal stem cells populations. The immune cell population, specifically T lymphocytes, may have a direct role in the secretion of pro-inflammatory cytokines that contribute to the characteristic tissue inflammation seen with adipose tissue excess.

Knee osteoarthritis, a disease that involves cartilage destruction and bone proliferation, is characterized by the acute inflammatory response that accompanies it. Although the proposed mechanisms play a significant role in the pathogenicity of the disease, other factors are believed to contribute to the severity of the disease. The infrapatellar fat pad (IPFP), located posterior to the patella, shares characteristics with other adipose depots throughout the body. Its secretory activity, specifically the release of pro-inflammatory cytokines, resembles that of adipose tissue depots. With this in mind, the infrapatellar fat pad may exacerbate the osteoarthritic condition and contribute to the etiology of the disease. This study analyzed the immunophenotype and differentiation potential of the infrapatellar fat pad in comparison to subcutaneous adipose tissue in order to determine its role in osteoarthritis and relationship to subcutaneous and visceral adipose tissue morphology.

Flow cytometry results revealed that cell populations present in the infrapatellar fat pad parallel those within subcutaneous adipose tissue. Both adipose depots exhibited similar levels of expression for the majority of markers including T cell, monocyte, and mesenchymal stem cell markers. However, analyses revealed a significant difference between the endothelial cell populations present in each depot. Subcutaneous adipose tissue showed a significantly higher endothelial marker expression, which can be accounted for by the decreased vascularity of the infrapatellar fat pad relative to subcutaneous adipose tissue.

The proliferation and differentiation ability of both adipose depots was examined and compared using a colony-forming unit assay. Results revealed similarities between the differentiation and proliferation of cell populations in subcutaneous adipose tissue and the infrapatellar fat pad, indicating that both depots share a similar composition. Adipose derived stem cells retrieved from both tissue samples were maintained in culture and further analyzed using flow cytometry.

Introduction

1.1 Function and Significance of Adipose Tissue in Tissue Inflammation

Adipose tissue is widely distributed throughout the human body. It not only functions as an endocrine organ, but also has anti-inflammatory and immuno-modulatory characteristics. Its secretion of trophic factors such as adiponectin and leptin effects other hormonal pathways in the body. In addition to secretory activity, it also possesses membrane bound receptors that respond to signals from other organs including the central nervous system. Its direct link with the central nervous system forms a feedback loop that regulates several biological processes including energy metabolism, neuroendocrine function, and immune function. Adipose tissue also exhibits a heterogeneous cell population. The Stromal Vascular Fraction (SVF), an isolated cell pellet obtained after digestion and centrifugation of a tissue sample, is composed of multiple cell lineages including adipocytes, endothelial cells, mesenchymal stem cells (MSCs), and leukocytes. T cells, a subset of leukocytes, recognize specific antigens using a specific cell surface antigen T cell receptor (TCR) (27). This recognition by T cells leads to the activation, proliferation, and secretion of cytokines and growth factors. These T cell populations reside in adipose tissue and contribute to the inflammatory condition observed with increased adipose tissue mass.

The growth factors leptin and adiponectin are believed to play a role in tissue inflammation. Leptin, a 16kDa polypeptide hormone encoded by the *obese* (*ob*) gene, is an adipokine secreted by adipocytes that regulates adipose tissue mass and body weight through a negative feedback loop with the hypothalamus (24). Mutations in either the *ob* gene or leptin receptor encoding *diabetes* (*db*) gene are associated with extreme obesity (24). In addition, leptin also stimulates the production of the cytokine Interleukin-1 beta (IL1β) to increase the production of pro-inflammatory cytokines. With its immunological function, leptin also aids in the activation of other leukocytes including neutrophils, macrophages, dendritic cells, natural killer cells, and T helper 1 cells (12). Adiponectin, a multifunctional protein released from adipocytes, regulates multiple biological pathways including insulin sensitivity, cell proliferation, tissue remodeling, and inflammation (19). Although claimed to have an anti-inflammatory function in obesity and vascular diseases, it may produce opposite effects and exacerbate inflammation seen in joint diseases such as osteoarthritis.

1.2 Pathology of Osteoarthritis and Significance of the IPFP in Osteoarthritis

The infrapatellar fat pad, also known as Hoffa's fat pad, is an intracapsular structure situated outside the synovial lining of the knee. Lying posterior to the patellar tendon and anterior to the knee joint, the fat pad extends from its attachment site on the inferior surface of the patella to the cartilage surrounding the anterior portion of the femur (3). Similar to subcutaneous adipose tissue, the Hoffa's fat pad is surrounded by a framework of fibrous cords that aid in vascularization of the region. The synovial fluid of the knee is situated between the synovial membrane and fat pad. This flexible, displaceable structure is believed to increase synovial surface area, aid in joint lubrication, and provide nutrients such as oxygen and protein to joint tissue (3, 20). The synovium is composed of multiple cell lineages, including antigen-producing leukocyte populations. These cells mediate the inflammatory response to injury or disease of the knee.

Osteoarthritis (OA) is an aberrant repair mechanism that involves the loss and subsequent synthesis of tissue following trauma. The disease itself, considered to be progressive and age-related, is characterized by cartilage destruction and abnormal bone remodeling (22). Osteoarthritis often involves an increase in subchondral bone mass and osteophyte growth in the joint periphery (24). This aberrant repair mechanism begins to exhibit significant pathology when tissue degradation far exceeds the synthesis of cartilage chondrocytes, extracellular matrix, and subchondral bone (2). Osteoarthritis of the knee occurs in all joint tissues including cartilage, bone, synovium, ligaments, and muscles (1). In addition to these components, the knee joint also contains adipose tissue: the infrapatellar fat pad (12). Considering the location of the IPFP within the knee joint and the secretory activity associated with adipose tissue, it is possible that the heterogeneous cell population comprising the patellar fat pad may contribute to the inflammation seen in knee osteoarthritis.

Experimental results have indicated that the inflammatory response of OA can be attributed to immune response exhibited by T cell populations (21). T cells are believed to play a significant role in the onset and progression of knee OA through pro-inflammatory cytokine release and subsequent activation of macrophage populations within adipose tissue (9,21). Recent studies have shown that T cells infiltrate the synovial membrane of the knee in osteoarthritis. The T cells interact with and activate several cell types including

macrophages, monocytes, chondrocytes, and osteoclasts either through soluble mediators or direct interaction. Soluble mediators such as IL-17 can signal the production of nitric oxide synthase in chondrocytes, which inhibits matrix synthesis and promotes degradation of cartilage (21). T cell activation can also contribute to joint destruction in OA by both inducing the production of collagenase, an enzyme responsible for cleaving peptide bonds in collagen, and triggering apoptosis of chondrocytes in the knee cartilage (21). Given its cellular composition and role in inflammation in other regions of the body, the infrapatellar fat pad may show characteristics analogous to that of the synovial membrane and other adipose depots.

1.3 Overview of Fluorescence Activated Cell Sorting (FACS)

FACS, also known as flow cytometry, is an assay that characterizes cells within a heterogeneous population based on light scattering properties (3). Flow cytometry integrates the basic principles of fluidics, optics, and electronics when sorting and analyzing samples. It measures the physical characteristics of cells suspended in a fluid sheath as they pass through a laser beam (4). A flow cytometer sorts cells based on several factors including size, internal structure, granularity, and fluorescent intensity (4). Prior to flow cytometry analysis, samples are stained with fluorochromes that absorb light energy over a range of wavelengths. This absorption of light excites an electron, and eventually results in the decay of an electron to a lower energy level and emission of energy as a photon of light. After staining, the sample enters the fluidics system, which transports particles in the fluid sheath to the laser beam for interrogation. The optics system, composed of a series of lasers, illuminates the samples and directs fluorescent light signals to detectors that convert light to electrical signals. The detectors convert the photons of light into electrical impulses, which are then relayed to an analog-to-digital converter. The converter translates the impulses into a numerical signal and produces data set showing the presence or absence of specific cell populations based on the number of excitation events of each fluorochrome.

1.4 Hypothesis and experimental design

The infrapatellar fat pad will exhibit cell populations similar to that of subcutaneous adipose tissue. To test this hypothesis, infrapatellar fat pad, subcutaneous adipose tissue, and blood serum samples were collected from osteoarthritic patients undergoing arthroscopy and/or total knee replacement. The samples were processed according to the experimental

protocol and stained with a specific panel of fluorochromes for flow cytometry analysis. In addition, lipoaspirate samples were evaluated using the same the fluorochrome panel. The proliferation and differentiation of IPFP and subcutaneous adipose tissue cells were also assessed using the colony forming unit and differentiation assay. Passage 2 adipose derived stem cells from donors used in the CFU assay were also stained and evaluated using a 9 fluorochrome panel. In addition, endothelial cell labeling and differentiation assays were incorporated later in the study to analyze tissue vascularization and ASC differentiation potential.

Materials and Methods

2.1 Tissue Harvest and Processing

Infrapatellar fat pad, subcutaneous adipose tissue, and blood serum samples were collected from osteoarthritic subjects (n=9 total, n=7 used for data set) undergoing arthroscopy and/or total knee replacement. All specimens were collected under protocol reviewed and approved by LSUHSC-NO or PBRC Institutional Review Board. The samples were transported to Pennington Biomedical Research Center on the day of the procedure. Both the infrapatellar fat pad and subcutaneous tissue sample weights were recorded prior to processing. The samples were first minced and washed 2-3 times with PBS prior to digestion. A volume of 2mL collagenase digest: 1g tissue (20 mL PBS, 20 μL 2mM Calcium Chloride, 20 mg Collagenase, 200 mg Albumin) was added to each tissue sample; the samples were then placed in a rocker dry oven at 37°C for 1 hour. Following digestion, the samples were centrifuged twice at 1200 RPM (300 g) for 5 minutes, filtered using a 100 μM filter, and centrifuged again at 1200 RPM (300 g) for 5 minutes to obtain the stromal vascular fraction (SVF). In order to remove erythrocytes from the sample and decrease the total number of events in flow cytometry analysis, 5 mL of a Red Blood Cell Lysis Buffer (200 mL distilled water, 1.66 g Ammonium Chloride, 0.2 g Pottassium Bicarbonate, 605 μL 0.25 EDTA) was used; 20 mL of PBS was added to terminate RBC lysis. After centrifugation at 1200 RPM (300 g) for 5 minutes, the supernatant was removed and the samples were resuspended in 5 mL of Stromal Medium (DMEM/F-12, 10% fetal bovine serum (FBS; Hyclone, Logan, UT), 1% antibiotic/antimycotic (MP Biomedicals, Solon, OH)). Following the processing procedure, 20μL of cell suspension from both samples was stained with Trypan Blue (Sigma) and counted using a hemocytometer. In addition to

samples from osteoarthritic patients, lipoaspirate samples (n=3) were collected and processed following a similar procedure.

2.2 Serum Analysis

Blood serum samples were collected from osteoarthritic subjects (n=10) and transported to the clinical chemistry laboratory at PBRC for further analysis (Table 1). The Homeostasis Model of Assessment- Insulin Resistance (HOMA-IR) was calculated as follows: fasting insulin (μU/mL) x fasting glucose (mg/dL)/405. All blood samples were collected from fasting glucose levels. In addition, 33.3% of the donors were diabetic and 66.7% were hypertensive, according to patient demographic sheets obtained from medical staff.

Donors (n=10)											Mean
BMI	29.7	34.0	29.2	34.5	26.6	25.7	33.2	22.3	30.4	31.5	29.7 ± 3.7
Kellergen-Lawrence Score	4.0	4.0	4.0	4.0	1.0	4.0	1.0	4.0	4.0	4.0	3.4 ± 1.2
Glucose(mg/dL)	108.0	140.0	102.0	125.0	95.0	126.0	90.0	118.0	131.0	119.0	115.4 ± 15.4
Cholesterol(mg/dL)	162.0	127.0	145.0	164.0	192.0	190.0	243.0	229.0	111.0	212.0	177.5 ± 41.2
HDL(mg/dL)	53.5	35.7	36.5	46.5	71.1	46.3	41.3	79.0	38.4	59.1	50.7 ± 14.1
LDL(mg/dL)	82.9	55.9	83.1	85.9	104.5	114.3	144.9	133.0	55.4	113.5	97.3 ± 28.6
HOMA-IR	1.5	2.0	1.0	1.4	1.4	0.6	2.6	3.6	2.1	1.7	1.8 ± 0.8
Insulin(μLU/mL)	5.5	5.8	3.8	4.4	5.8	2.0	11.9	12.3	6.6	5.8	6.4 ± 3.1
Triglyceride(mg/dL)	128.0	177.0	127.0	158.0	82.0	147.0	284.0	85.0	86.0	197.0	147.1 ± 59.0

Table 1: Donor Demographics and Serum Analysis

2.3 Fluorescence Activated Cell Sorting (FACS) Staining Procedure

After the processing procedure, the samples were prepared for flow cytometry analysis according to the provided staining protocol. If necessary, the samples were diluted to the required concentration of $1x10^6$ cells per mL. The cells were washed in 10 mL PBS and centrifuged twice at 1200 RPM for 5 minutes, then resuspended in 500 μL cold PBS. The sample was transferred to a 1.5 mL microcentrifuge tube containing the 87 μL mixture of the 13 fluorochrome panel (Table 2). The stained samples were incubated in a dark environment at room temperature for 30 minutes. The cells were then washed with 1 mL PBS and 1% BSA and centrifuged at 300xg for 3 minutes three times. They were resuspended in 500 μL of 1%

formaldehyde in PBS, stored at 4°C, and transported to LSUHSC-NO within 48 hours for flow cytometry analysis.

Fluorochrome	Marker	Volume per test	Catalog Number and Company
PerCP Cy5.5	CD14	5 microliters	45-0198-42 (eBioscience, San Diego, CA)
FitC	CD31	5 microliters	11-0319-42 (eBioscience, San Diego, CA)
Qdot	CD8	1 microliter	Q10055 (Invitrogen, Carlsbad, CA)
PE Cy7	CD34	5 microliters	25-0349-42 (eBioscience, San Diego, CA)
PE Cy5	CD38	5 microliters	15-0389-42 (eBioscience, San Diego, CA)
eFluor 450	CD16	5 microliters	48-0168-42 (eBioscience, San Diego, CA)
APC	CD66abce	10 microliters	130-093-155 (Miltenyi Biotec Inc., Auburn, CA)
v500	CD4	5 microliters	560768 (Becton, Dickinson, and Company, Franklin Lakes, NJ)
APC Cy7	CD25	5 microliters	557753 (Becton, Dickinson, and Company, Franklin Lakes, NJ)
ECD	CD20	10 microliters	PNIM3607U (Beckman Coulter, Brea, CA)
Alexa Fluor 700	CD56	25 microliters	557919 (Becton, Dickinson, and Company, Franklin Lakes, NJ)
Qdot 655	CD3	1 microliter	Q10054 (Invitrogen, Carlsbad, CA)
PE	CD29	5 microliters	12-0299-71 (eBioscience, San Diego, CA)

Table 2: Fluorochrome Panel

2.4 Colony-forming unit (CFU) assay

Cells within the SVF of the infrapatellar fat pad and subcutaneous adipose tissue samples (n=6) were processed and cultured for fibroblast (CFU-F), adipocyte (CFU-Ad), and osteoblast (CFU-ALP) differentiation according to published methods (Kozak et al 2009). After processing, the cells were seeded in T25 flasks with Stromal medium (DMEM/F-12, 10% fetal bovine serum (FBS; Hyclone, Logan, UT), 1% antibiotic/antimycotic (MP Biomedicals, Solon,

OH)) and incubated at 37°C in a 5% CO_2 humidified incubator until confluent. Once confluent, the cells were removed from the flasks with 0.25% Trypsin in 1mM ethylene diamine tetraacetic acid (EDTA) (Sigma), stained with 0.4% Trypan Blue (Sigma), and counted using a hemocytometer. The samples were then diluted concentrations of 100 and 50 cells per mL. The specified dilutions for the IPFP and subcutaneous adipose tissue samples were then transferred to a 6-well plate, seeded at 1 ml per well (50 or 100 cells total) (Figure 1). After 7 days in culture, the samples were induced with Stromal, Adipogenic ((DMEM/F-12, 3% FBS, 1% antibiotic/antimycotic, 33μM Biotin, 17μM Pantothenate, 1μM Insulin, 1μM Dexamethasone, 0.5mM IBMX, 5 μM Rosiglitazone (AK Scientific, Mountain View, CA)), or Osteogenic (DMEM/F-12, 10% FBS, 1% antibiotic/antimycotic, 10 mM β-Glycerophosphate, 0.1 μM Dexamethasone, 50 ng/ml Ascorbic Acid 2-Phosphate) differentiation media and maintained in culture for 9 days. On day 9, the observed colonies were fixed and stained following the fibroblast, adipocyte, and Alkaline Phosphatase staining protocols.

For the CFU-F assay, the cells were rinsed twice with warm phosphate-buffered saline (PBS) and fixed with 10% formalin for 20 minutes at room temperature. The cells were then stained for 1 hour with 0.1% Toluidine blue in 1% paraformaldehyde in PBS. Stained cells were gently rinsed with distilled water twice and photographed using a computer scanner.

For the CFU-Ad assay, the cells were then fixed for 1 hour with 10% formalin at room temperature and stained with Oil red O for 20 minutes. The plate was scanned immediately following the removal of the staining solution using a computer scanner.

For the CFU-ALP assay, the cells were rinsed once with PBS and placed in 95% ethanol at 4°C for 10 minutes. After the alcohol was removed, the plate air-dried for 5 minutes. The cells were then stained with Alkaline Phosphatase solution (0.46 mM 5-bromo-4-chloro-3-indolyl phosphate, 1.2 mM Nitroblue Tetrazolium, 8.3 Magnesium Sulfate, 36 mM Sodium Metaborate pH 9.2) and incubated at 37°C in a 5% CO_2 humidified incubator overnight. The samples were monitored for a color reaction, then rinsed with PBS and photographed following completion.

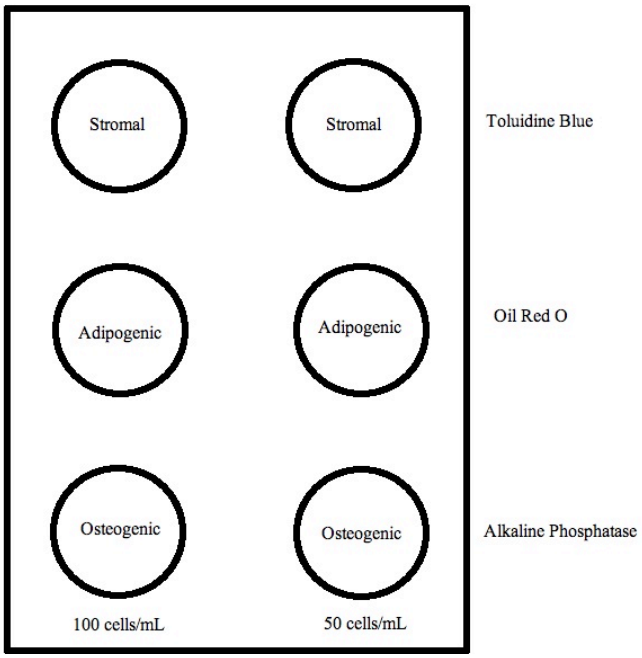

Figure 1: Samples were diluted to 100 and 50 cells/mL concentrations and plated in 6-well plates. After 7 days in culture, the wells were either maintained in stromal medium or induced with adipocycte or osteoblast differentiation medium. The colonies were then stained after 9 days of induction.

2.5 Fluorescence Activated Cell Sorting (FACS) Staining of expanded cells

The infrapatellar fat pad and subcutaneous adipose tissue samples of osteoarthritic patients (n=7 IPFP, n=6 Subcutaneous) were processed according to the experimental protocol. After collagenase digestion and centrifugation, cells from the stromal vascular fraction (SVF) were seeded in T25 flasks with Stromal medium (DMEM/F-12, 10% fetal bovine serum (FBS; Hyclone, Logan, UT), 1% antibiotic/antimycotic (MP Biomedicals, Solon, OH)) and incubated at 37°C in a 5% CO_2 humidified incubator. The stromal medium was changed daily and the flasks remained in incubation until the cells were confluent and reached passage 2. The cells were then removed from the flasks with Trypsin, resuspended in stromal medium, and counted using a hemocytometer. The samples were stained for flow cytometry following the provided protocol.

2.6 Endothelial Cell Labeling

A nickel size piece of tissue was sectioned from subcutaneous adipose tissue and infrapatellar fat pad samples (n=3) and transferred to a 1.5 mL microcentrifuge tube. 1 mL of stock solution of isolectin (500 mg/mL) was diluted to 10 µg/mL and transferred to each sample.

The sections were then incubated in the dark for 1 hour with the lectin fluoresceinisothiocyanate (FITC) conjugate from *Ulex europaeus* (Sigma Aldrich). Samples were then washed with PBS and analyzed with a confocal microscope. Vessel density was determined by superimposing an image of each sample on a grid using ImageJ software. Vessel density is defined as the number of times a vessel intersects a gridline within the specified area.

2.7 Cell Differentiation Assay

The infrapatellar fat pad and subcutaneous adipose tissue samples of osteoarthritic patients (n=3) were processed according to the experimental protocol. After collagenase digestion and centrifugation, cells from the stromal vascular fraction (SVF) were seeded in 12-well plates with stromal medium (DMEM/F-12, 10% fetal bovine serum (FBS; Hyclone, Logan, UT), 1% antibiotic/antimycotic (MP Biomedicals, Solon, OH)) and incubated in at 37°C in a 5% CO_2 humidified incubator. The stromal medium was changed daily and the plates remained in incubation until the cells were confluent. Passage 1 ASCs were then seeded in either T25 or T75 flasks until confluent. Once confluent, passage 2 ASCs were washed with PBS, removed with Trypsin, and counted using a hemocytometer. After counting, samples were centrifuged at 1200 RPM (300 g) for 5 minutes and resuspended in stromal medium at a concentration of $1.5x10^6$ cells/mL. After adding 1mL/well of stromal media to a12-well plate, 1 mL of the sample was aliquoted to each well. The plates were then incubated at 37°C in a 5% CO_2 humidified incubator for 3 days, then induced with Stromal, Adipogenic ((DMEM/F-12, 3% FBS, 1% antibiotic/antimycotic, 33μM Biotin, 17μM Pantothenate, 1μM Insulin, 1μM Dexamethasone, 0.5mM IBMX, 5 μM Rosiglitazone (AK Scientific, Mountain View, CA)), or Osteogenic (DMEM/F-12, 10% FBS, 1% antibiotic/antimycotic, 10 mM β-Glycerophosphate, 0.1 μM Dexamethasone, 50 ng/ml Ascorbic Acid 2-Phosphate) differentiation media and maintained in culture for 12 days. On day 12, the samples were fixed and stained following the Oil Red O and Alizarin Red staining protocols. RNA from 8 of the 12 wells was harvested for further PCR analysis.

Results

3.1 Cell surface receptor characterization of the infrapatellar fat pad and subcutaneous adipose tissue

Flow cytometric analyses of the infrapatellar fat pad and subcutaneous adipose tissue indicate a significant difference in CD31 expression (r^2=0.021, $P < 0.05$). Compared to the infrapatellar fat pad, subcutaneous adipose tissue displayed increased expression the endothelial cell marker, CD31 (Figure 2). Lower levels of CD31 in the infrapatellar fat pad in comparison to subcutaneous adipose tissue can be explained by the avascularization that is associated with the fat pad region of the knee. With the exception of CD31, no significant difference was noted in cell populations between the two depots for levels of expression of the selected panel of immune and mesenchymal cell markers (Table 3; Figure S-1; Figure S-2). The T-cell markers, including CD3, CD4, CD8, and CD25 were comparable.

Depot	Marker	Mean	P Value
Subcutaneous	CD14 %Parent	22.9 ± 8.2	0.39
Fat Pad	CD14 %Parent	17.9 ± 13.6	
Subcutaneous	CD29+ %Parent	42.6 ± 20	0.27
Fat Pad	CD29+ %Parent	34.1 ± 30.2	
Subcutaneous	CD31 %Parent	22.3 ± 7.8	0.02
Fat Pad	CD31 %Parent	9.9 ± 5.1	
Subcutaneous	CD56 %Parent	16.2 ± 12.1	0.29
Fat Pad	CD56 %Parent	7.2 ± 10.8	
Subcutaneous	CD3 %Parent	11.8 ± 9.6	0.28
Fat Pad	CD3 %Parent	6.6 ± 4.5	
Subcutaneous	CD3+CD8+ %Parent	12.8 ± 13.7	0.64
Fat Pad	CD3+CD8+ %Parent	10.7 ± 13.1	
Subcutaneous	CD16 %Parent	12.8 ± 9.6	0.50
Fat Pad	CD16 %Parent	8.6 ± 13.9	
Subcutaneous	CD66 %Parent	6.6 ± 12	0.25
Fat Pad	CD66 %Parent	0.4 ± 0.3	
Subcutaneous	CD20 %Parent	0.8 ± 1.7	0.32
Fat Pad	CD20 %Parent	0.2 ± 0.4	

Table 3: Comparison of IPFP and Subcutaneous Adipose Tissue Marker Expression

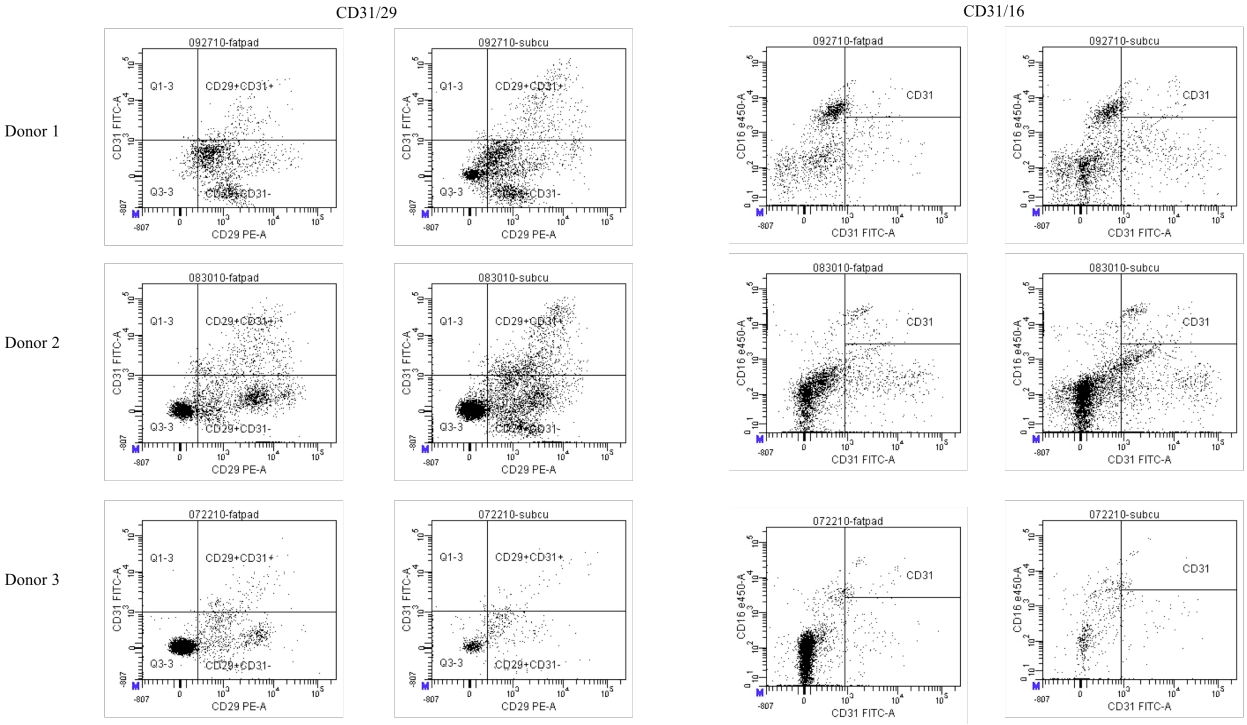

Figure 2: FACS Analysis of the Infrapatellar Fat Pad (IPFP) in comparison to Subcutaneous Adipose Tissue

3.2 Cell surface receptor characterization of lipoaspirate samples

Flow cytometric analyses of the lipoaspirate samples obtained from an independent set of subjects undergoing elective cosmetic surgery (n = 3) revealed results similar to that of subcutaneous adipose tissue from subjects undergoing total knee replacement (Table 4). Both samples exhibited similar expression of specific markers, indicating that populations present in lipoaspirate parallel those found in subcutaneous adipose tissue. Statistical analysis of the data sets further confirmed an insignificant difference between the lipoaspirate and subcutaneous adipose tissue samples.

Sample	Marker	Mean	P value
Lipoaspirate	CD14 %Parent	26.1 ± 11.8	0.60
Subcutaneous	CD14 %Parent	22.1 ± 10.4	
Lipoaspirate	CD16 %Parent	8.9 ± 4.4	0.83
Subcutaneous	CD16 %Parent	10.7 ± 11.5	
Lipoaspirate	CD56 %Parent	8.8 ± 6.9	0.16
Subcutaneous	CD56 %Parent	20.2 ± 13.0	
Lipoaspirate	CD31 %Parent	26.7 ± 13.4	0.52
Subcutaneous	CD31 %Parent	20.7 ± 5.6	
Lipoaspirate	CD29+ %Parent	45.8 ± 19.8	0.41
Subcutaneous	CD29+ %Parent	31.9 ± 13.8	

Table 4: Comparison of Lipoaspirate Samples to Subcutaneous Adipose Tissue

3.3 IPFP and subcutaneous adipose tissue cell proliferation and differentiation

For the CFU assay, passage 1 cells from the infrapatellar fat pad and subcutaneous adipose tissue were plated at densities of 50 and 100 cells/mL. After 7 days in culture, cells were induced to undergo osteogenesis and adipogenesis or maintained to form the characteristic fibroblast. The CFU counts were then determined through histochemical staining of each of the plates. The average number of colonies from IPFP samples did not exhibit a significant difference between the fibroblast and osteoblast assay (Table 5; Figure 6). Furthermore, cells plated at a lower density of 50 cells/mL displayed greater colony formation relative to cells plated at 100 cells/mL. The average colony counts of subcutaneous adipose tissue samples for CFU-F and CFU-ALP assays were comparable and showed little variation in colony formation (Table 6; Figure 5). However, deviation still exists between plating densities; cells seeded at lower densities showed a greater ability to generate colonies in comparison to those seeded at higher densities. Statistical analysis of colony formation and differentiation ability of cells from both depots revealed only numerical significant differences (Table 7). The number of colonies formed between the two depots differed, however their differentiation ability parallels one another (Figure 4). Cells from both depots are able to differentiate into osteoblast and fibroblast lineages after induction (Figure 3). Unlike CFU-F and CFU-ALP assays, cells induced to

undergo adipogenesis did not exhibit proliferation or differentiation. As a result, an adipocyte colony count was not obtained.

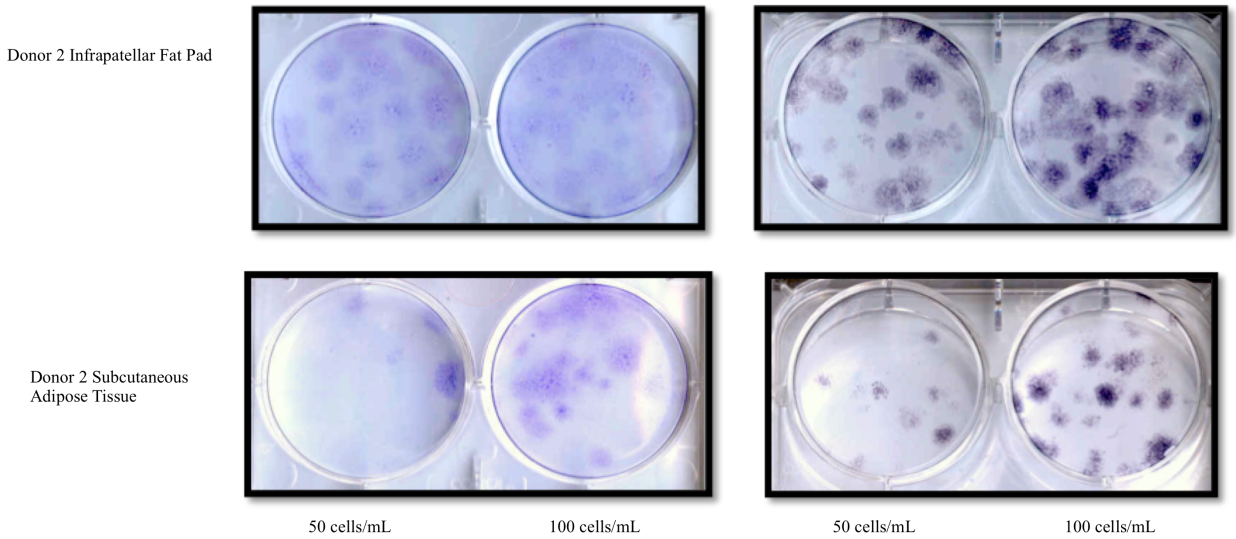

Figure 3: Comparison of Infrapatellar Fat Pad (IPFP) and Subcutaneous Adipose Tissue Colony Forming Units at densities of 50 cells/mL and 100 cells/mL

IPFP		
Concentration (cells/mL)	Mean Stromal	Mean Osteo
50	40 ± 8.1	36.1 ± 16.3
100	23.3 ± 4.9	25.7 ± 8.4

Table 5: IPFP CFU-F and CFU-ALP colony count plated at concentrations of 50 and 100 cells/mL

Subcutaneous Adipose Tissue		
Concentration (cells/mL)	Mean Stromal	Mean Osteo
50	23.0 ± 10.7	24.8 ± 10.2
100	17.5 ± 3.9	18.8 ± 6.0

Table 6: Subcutaneous Adipose Tissue CFU-F and CFU-ALP colony count plated at concentrations of 50 and 100 cells/mL

T-Test (IPFP vs. Subcutaneous)	
Stain and Concentration (cells/mL)	P value
CFU-F (50)	1.50E-05
CFU-ALP (50)	1.56E-02
CFU-F (100)	4.01E-04
CFU-ALP (100)	7.02E-03

Table 7: Statistical comparison of IPFP and subcutaneous adipose tissue colony counts for CFU-F and CFU-ALP assays at concentrations of 50 and 100 cells/mL

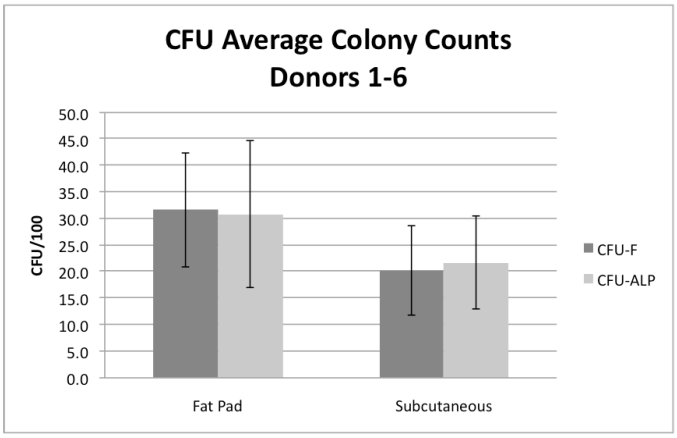

Figure 4: CFU Average Colony Counts

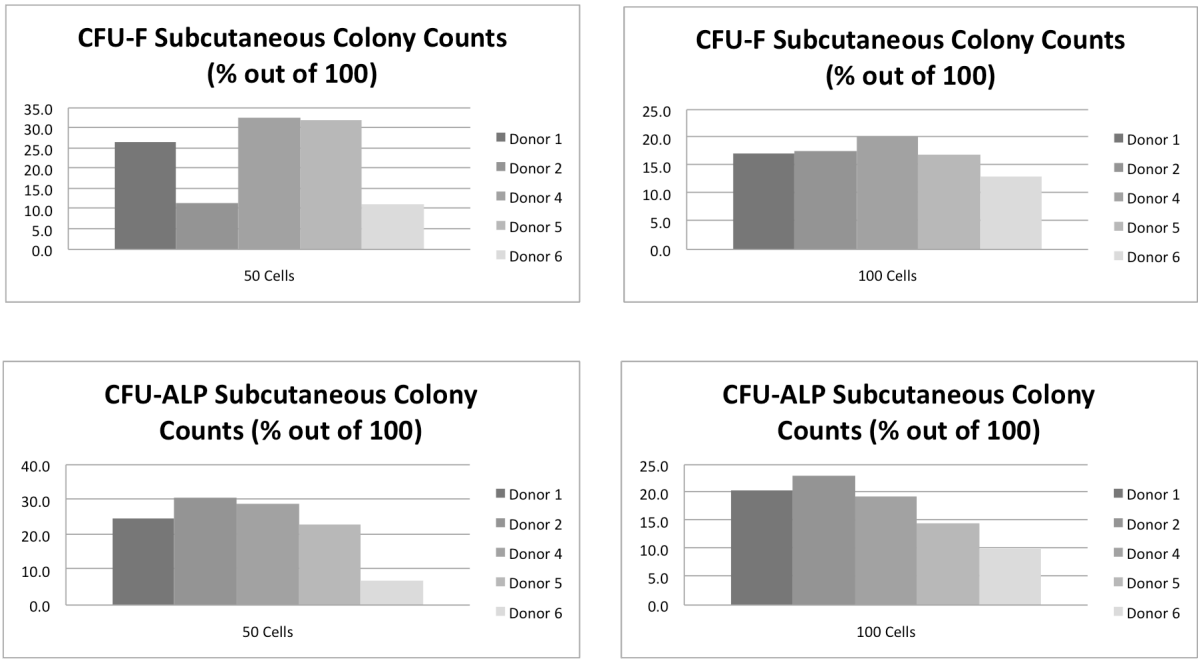

Figure 5: CFU Subcutaneous Adipose Tissue Colony Counts

Figure 6: CFU IPFP Colony Counts

3.4 Cell Surface Marker Expression of ASCs

Passage 1 cells from IPFP and subcutaneous adipose tissue samples were maintained in culture until confluent. After confluence was achieved, the cells were either plated in a 6-well plate for the CFU assay or seeded in a T175 flask to undergo passage 2. Passage 2 adipose derived stem cells were then maintained in culture until confluent. Once confluent, the ASCs were stained with the specified panel of fluorochromes for flow cytometry analysis (Table 8). Results showed that ASCs from IPFP and subcutaneous adipose tissue parallel one another. In addition, there was no statistically significant difference in marker expression between ASCs from the two depots.

Fluorochrome	IPFP Mean	Subcu Mean	P Value
huCD29	85.9 ± 35.6	95.6 ± 8.5	0.51
huCD105	99.5 ± 0.3	99.2 ± 0.8	0.50
huCD45	4.4 ± 3.5	4.9 ± 4.1	0.97
huCD34	17.2 ± 12.7	12.8 ± 8.7	0.15
huCD44	74.0 ± 7.9	57.0 ± 22.9	0.07
huCD73	99.4 ± 0.6	99.4 ± 0.5	0.85
huCD90	99.6 ± 0.3	99.7 ± 0.2	0.28
PE IgG1	7.3 ± 7.3	8.3 ± 5.7	0.94
FITC IgG1	4.8 ± 2.3	9.5 ± 10.4	0.34
Control	1.9 ± 1.2	3.0 ± 3.1	0.72

Table 8: Comparison of Passage 2 ASC Marker Expression of IPFP and Subcutaneous Adipose Tissue

3.5 Endothelial Cell Labeling

Imaging of the stained infrapatellar fat pad and subcutaneous adipose tissue samples revealed increased vascularization of subcutaneous adipose tissue relative to the IPFP (Figure 7). After determining vessel intersections in a grid layout, subcutaneous adipose tissue exhibited approximately a 30 % increase in intersections relative to the IPFP. These results further support the characterization of the IPFP as an avascular region.

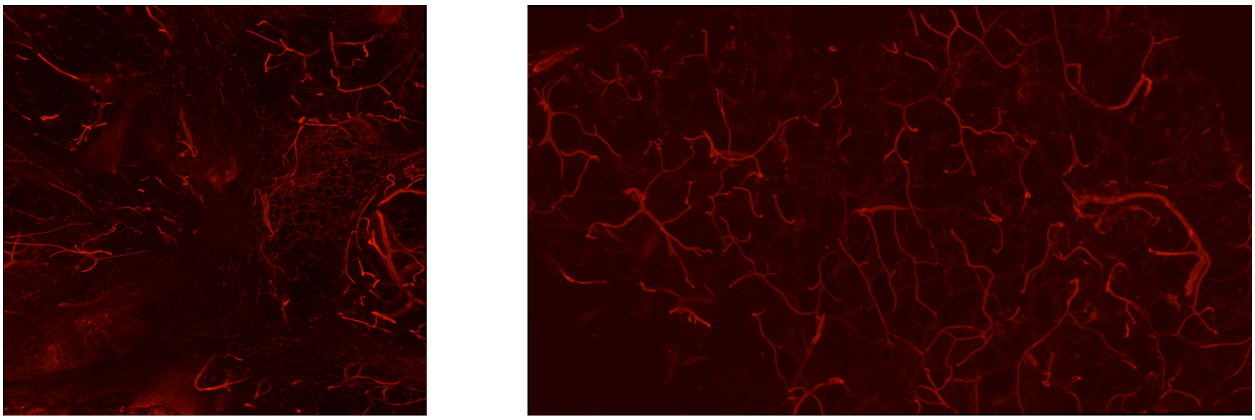

Infrapatellar Fat Pad

Subcutaneous Adipose Tissue

Figure 7: Endothelial Cell Labeling of IPFP and Subcutaneous Adipose Tissue. Subcutaneous adipose tissue displays a greater blood vessel density relative to IPFP samples

3.6 IPFP and Subcutaneous adipose tissue cell differentiation

Adipose-derived ASCs from the infrapatellar fat pad and subcutaneous adipose tissue exhibited differentiation potential following induction. When maintained in stromal medium, ASCs displayed fibroblast morphology. Furthermore, in the presence of adipogenic or osteogenic medium, ASCs differentiated into adipocyte and osteoblast cell lineages. These results are similar to the findings from previous studies with subcutaneous derived cells.

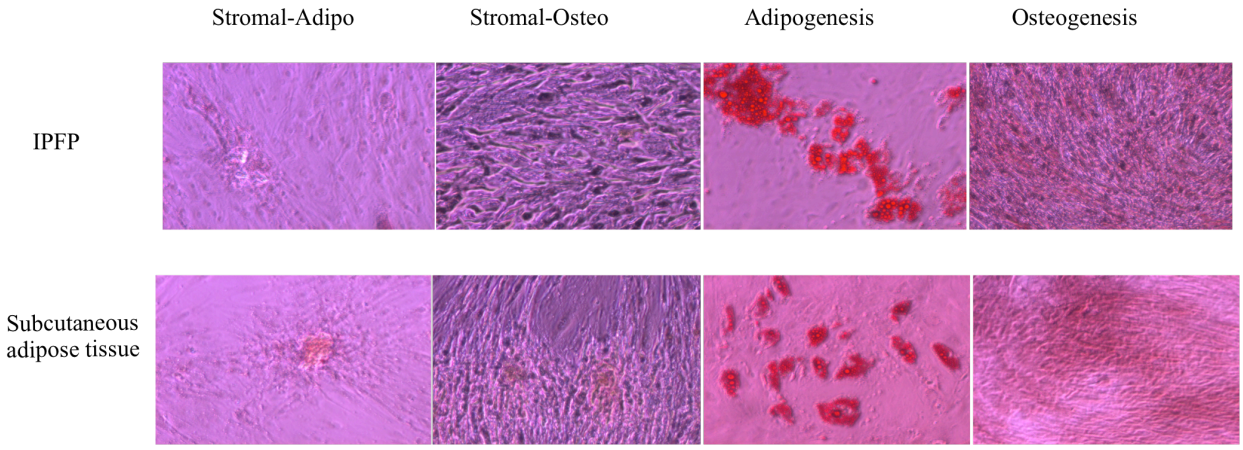

Figure 8: Adipose-derived ASCs were either maintained in Stromal medium or induced with adipogenic or osteogenic medium. After 12 days, the fibroblast, adipocyte, and osteoblast lineages were stained with Oil Red O and Alizarin Red.

Discussion

4.1 Quantitative differences contribute to distinction between the infrapatellar fat pad, subcutaneous adipose tissue, and visceral adipose tissue

The infrapatellar fat pad (IPFP) and subcutaneous adipose tissue exhibit similar marker expression and parallel one another in terms of cell morphology and quantity. Although both depots possess cell types similar to that of visceral adipose tissue, the population number and impact of that population within a specific region drastically differ (Table 9). Dr. Hyunwon Yang and colleagues showed that when comparing the inguinal fat pad, pelvic subcutaneous adipose tissue (SAT), to visceral adipose tissue (VAT), $CD8^+$ cells showed elevated expression, whereas SAT only exhibited an increase in $CD4^+$ T cells (9). Visceral adipose tissue houses primarily effector-memory (E/M) T cells, as opposed to subcutaneous adipose tissue, which is composed mainly of naïve T cells (9). The E/M phenotype T cells produce excessive amounts of pro-inflammatory cytokines, which contributes to the acute inflammatory condition seen in VAT. In addition, E/M T cells assist in the recruitment and infiltration of macrophages into the adipose depot. Macrophages then initiate an inflammatory cascade that consequently causes inflammation (25). Although IPFP and subcutaneous adipose tissue exhibited lower levels of expression of CD8 and CD4, studies have shown that specifically activated T cells infiltrate the synovial membrane (located on the outer surface of the infrapatellar fat pad) of OA patients (26). Data from a study by Sakkas et al. indicates that T cell aggregates were found in 65% of patients with OA (27). There are mixed results with regards to whether TH1 or TH2 predominate the T cell population within the synovial membrane (27). TH1 cells are responsible for the release of interleukin 2 and gamma interferon, whereas TH2 cells are associated with the release of interleukin 4 and 5. The cytokines IL-2 and IFN-γ secreted from TH1 cells are expressed in the synovium of OA patients, which would support a cell-mediated immune response as a key factor in the onset of osteoarthritis (21,27). Although the synovium exhibits pro-inflammatory characteristics associated with T cell populations, the role of the IPFP in terms of osteoarthritis and chronic inflammation remains unclear.

4.2 Obesity and its role in osteoarthritis

Obesity is one of the largest, most preventable risk factors for the development of osteoarthritis (23). The relationship between obesity and osteoarthritis has been extensively

studied, but conclusive evidence of a direct or indirect relationship between the two conditions has yet to be established (22, 24). Specifically in the knee joint, obesity increases the risk of developing osteoarthritis from two-fold to ten-fold (22, 23). Biomechanical factors of the knee joint associated with body mass index, limb alignments, and quadriceps muscle strength contribute to the onset and progression of the disease, but do not explain the reasoning behind the occurrence of osteoarthritis in non-load bearing joints such as those of the hand (22, 23, 24). Obesity is characterized as a mild, chronic inflammatory disease. An increase in adipose tissue mass often results in adipocyte necrosis, which then leads to the infiltration of activated macrophages and concurrent production of pro-inflammatory cytokines and cytokine-like molecules (adipokines or cytokines such as leptin, TNFα, IL-1, and IL-6) (22, 23). The secretion of pro-inflammtory cytokines from adipose tissue provides a possible non-biomechanical link between obesity and osteoarthritis (22).

Elevated levels of pro-inflammatory cytokines can stimulate catabolic processes in chondrocytes in vitro, resulting in extracellular matrix degradation of the articular cartilage (22). Recent studies have focused on one adipokine in particular, leptin. Leptin alters chondrocyte matrix metabolism and up-regulates catabolic and anabolic activities, which is consistent with the cellular alterations exhibited in osteoarthritis (22, 24). Leptin's most profound characteristic is its ability to mediate both metabolic and inflammatory processes (22, 23, 24). In a recent study, Otero and colleagues demonstrated that the simultaneous stimulation of chondrocytes with leptin and interleukin-1 or interferon-γ resulted in increased expression of inducible nitric oxide synthase, an enzyme responsible for the production of nitric oxide and citrulline from arginine, molecular oxygen, and nicotinamide adenine diphosphate (24, 28, 29). Increased production of nitric oxide amplifies the effects of IL-1 on joint degradation by decreasing matrix synthesis and up-regulating metalloprotease protein degradation activity (24).

Griffin and colleagues have conducted a number of research studies concerning the effects of diet, extreme obesity, and leptin activity on knee osteoarthritis. Results have shown that extremely obese leptin-impaired mice do not develop an increased incidence of knee osteoarthritis, suggesting that severe obesity is not the direct cause of osteoarthritis. Adiposity alone, in the absence of leptin activity, is unable to induce systemic inflammation associated with osteoarthritis. Murine models only exhibited altered levels of leptin when given a high-fat diet. A strong association exists between leptin and disease severity, indicating that leptin is the target

for osteoarthritis in obese patients. Furthermore, physiological levels of leptin do not alter extracellular matrix homeostasis of healthy cartilage, but only specifically target osteoarthritic tissue. The strong association between leptin and osteoarthritis opens up the door to a number of treatment possibilities including a pharmacological approach. Pro-inflammatory cytokines IL-1, IL-6, IL-8, TNF-α, and prostaglandin E_2, all byproducts of increased leptin levels, are possible targets for the prevention and treatment of obesity-induced osteoarthritis (22).

Marker	Cell Population(s)
CD3	T cell
CD4	helper T cell, peripheral blood monocyte, tissue macrophage, granulocyte
CD5	T cell, B cell
CD8	cytotoxic T cell
CD14	Monocyte, myeloid, osteoclast
CD16	NK cell, macrophage, monocyte, mast cell, T cell
CD20	B cell, T lymphocyte
CD25	regulatory T cell, B cell, monocyte, macrophage
CD29	mesenchymal stem cell, memory T cell, granulocyte
CD31	endothelial
CD34	hematopoietic cell, bone marrow stromal cell, capillary endothelium, embryonic fibroblast
CD38	erythroid, lymphoid, myeloid, early B and T cell, activated T cell, germinal center B cell, plasma cell, NK cell
CD56	NK cell
CD66a	granulocyte, epithelial cell, NK cell, LAK and activated T cell
CD66b	granulocyte
CD66c	granulocyte, epithelial cell
CC66e	epithelial cell

Table 9: Complementary Determinant Region and Representative Cell Populations

References

1. Osteoarthritis: National Clinical Guideline for Care and Management in Adults. London: Royal College of Physicians, 2008.
2. Moskowitz, RW, Altman RD, Hochberg MC, Buckwalter JA, Goldberg VM. Osteoarthritis: Diagnosis and Medical/Surgical Management. Philadelphia: Lippincott Williams and Wilkins, 2007.
3. Saddik D, McNally EG, Richardson M. "MRI of Hoffa's fat pad". *Skeletal Radiology* (2004): 433-444.
4. Macey, MG. *Flow Cytometry: Principles and Applications*. Totowa: Humana Press, 2007.
5. *Introduction to Flow Cytometry: A Learning Guide*. San Jose: BD Biosciences, 2000.
6. Fantuzzi G, Mazzone T. *Adipose Tissue and Adipokines in Health and Disease*. Totowa: Humana Press, 2007.
7. Gimble JM, Floyd EZ. "Fat Circadian Biology". *Journal of Applied Physiology* (2009): 1629-37.
8. Kershaw EE, Flier JS. "Adipose Tissue as an Endocrine Organ". *Journal of Clinical Endocrinology and Metabolism* (2004): 2548-56.
9. Hyunwon Y, Youm YH, Vandanmagsar B, Ravussin A, Gimble JM, Greenway F, Stephens JM, Mynatt RL, Dixit VD. "Obesity Increases the Production of Proinflammatory Mediators from Adipose Tissue T Cells and Compromises TCR Repertoire Diversity: Implications for Systemic Inflammation and Insulin Resistance". *Journal of Immunology* (2010): 1836-45.
10. Clements KM, Ball AD, Jones HB, Brinckmann S, Read SJ, Murray F. "Cellular and histopathological changes in the infrapatellar fat pad in monoiodoacetate model of osteoarthritis pain". *Osteoarthritis and Cartilage* (2009): 805-12.
11. Khan WS, Tew SR, Adesida AB, Hardingham TE. "Human infrapatellar fat pad-derived stem cells express the pericyte marker 3G5 and show enhanced chondrogenesis after expansion in fibroblast growth factor-2". *Arthritis Research and Therapy* 10. 4 (2008): R74
12. Clockaerts S, et al. "The infrapatellar fat pad should be considered as an active osteoarthritic joint tissue: a narrative review". *Osteoarthritis and Cartilage* 18. S2 (2010): S32.
13. Zola H, Swart B, Nicholson I, Voss E. *Leukocytes and Stromal Cell Molecules: The CD Markers*. John Wiley and Sons, Inc: Hoboken, 2007.
14. Myers, Robert A. *Immunology: From Cell Biology to Disease*. Wiley-VCH Verlag GmbH & Co. KGaA: Weinheim, 2007.
15. Tuan R, Boland G, Tuli R. "Adult mesenchymal stem cells and cell-based tissue engineering". *Arthritis Research and Therapy* 2003: 32-45.
16. Prockop DJ, Phinney DG, Bunnell BA. *Mesenchymal Stem Cells: Methods and Protocols. Methods in Molecular Biology*. Humana Press: Totowa, 2008.
17. Yang, K. "Adipose Tissue Protocols". *Methods in Molecular Biology*. Humana Press.
18. Staszkiewicz J, Frazier TP, Rowan BG, Bunnell BA, Chiu ES, Gimble JM, Gawronska-Kozak B. "Cell Growth Characteristics, Differentiation Frequency, and Immunophenotype of Adult Ear Mesenchymal Stem Cells". *Stem Cells and Development* 19 (2009): 83-92.

19. Fantuzzi G, Mazzone T, eds. *Adipose Tissue and Adipokines in Health and Disease*. Humana Press: Totowa, 2007.
20. Vigorita, Vincent J. *Orthopaedic Pathology*. 2nd Ed. Lippincott Williams and Wilkins: Philadelphia, 2008.
21. Sakkas LI, Platsoucas CD. "The Role of T Cells in the Pathogenesis of Osteoarthritis". *Arthritis and Rheumatism* (2007).
22. Griffin TM et al. "Diet-induced obesity differentially regulates behavioral, biomechanical, and molecular risk factors for osteoarthritis in mice". *Arthritis Research and Therapy* (2010): R130.
23. Griffin TM, Guilak F. "Why is obesity associated with osteoarthritis? Insights from mouse models of obesity". *Biorheology* (2008): 387-398.
24. Griffin TM et al. "Extreme obesity due to impaired leptin signaling in mice does not cause knee osteoarthritis". *Arthritis and Rheumatism* (2009): 2935-2944.
25. Nishimura S et al. "CD8+ effector T cells contribute to macrophage recruitment and adipose tissue inflammation in obesity". *Nature Medicine* (2009): 914-920.
26. Sakkas, L. I., C. Scanzello, N. Johanson, J. Burkholder, A. Mitra, P. Sal- game, C. D. Katsetos, and C. D. Platsoucas. "T cells and T-cell cytokine transcripts in the synovial membrane in patients with osteoarthritis". *Clinical and Diagnostic Laboratory Immunology* (1998): 430–437.
27. Liossis SN, Tsokos GC. "Cellular Immunity in Osteoarthritis: Novel Concepts for an Old Disease". *Clinical and Diagnostic Laboratory Immunology* (1998): 427-429.
28. Otero M, Gomez Reino JJ, Gualillo O. "Synergistic induction of nitric oxide synthase type II: in vitro effect of leptin and interferon-gamma in human chondrocytes and ATDC5 chondrogenic cells". *Arthritis and Rheumatism* (2003): 404-409.
29. Otero M, Lago R, Lago F, Reino JJ, Gualillo O. "Signaling pathway involved in nitric oxide synthase type II activation in chondrocytes: synergistic effect of leptin with interleukin-1". *Arthritis Research Therapy* (2005): R581-591.
30. Wickham MQ, Erickson GR, Gimble JM, Vali TP, Guilak F. "Multipotent stromal cells derived from the infrapatellar fat pad of the knee". *Clinical Orthopaedics and Related Research* 412 (2003): 196-212.
31. Dragoo JL, Lieberman JR, Lee RS, Deugarte DA, Lee Y, Zuk PA, Hendrick MH, Benhaim P. "Tissue-engineered bone from BMP-2 transduced stem cells derived from human fat". *Plastic and Reconstructive Surgery* 115.6(2005): 1665-73.
32. Vinardell T, Buckley CT, Thorpe SD, Kelly DJ. "Composition-function relations of cartilaginous tissues engineered from chondrocytes and mesenchymal stem cells isolated from bone marrow and infrapatellar fat pad". *Journal of Tissue Engineering and Regenerative Medicine* (2010).
33. Toghraie FS, Chenari N, Gholipour MA, Faghih Z, Torabineiad S, Dehghani S, Ghaderi A. "Treatment of osteoarthritis with infrapatellar fat pad derived mesenchymal stem cells in Rabbit". *Knee* (2010).
34. Buckley CT, Vinardell T, Thorpe SD, Haugh MG, Jones E, McGonagle D, Kelly DJ. "Functional properties of cartilaginous tissues engineered from infrapatellar fat pad-derived mesenchymal stem cells". *Journal of Biomechanics* 43.5 (2010): 920-5.
35. Jurgens WJ, van Dijk A, Doulabi BZ, Niessen FB, Ritt MJ, van Milligen FJ, Helder MN. "Freshly isolated stromal cells from the infrapatellar fat pad are suitable for a

one-step surgical procedure to regenerate cartilage tissue". *Cytotherapy* 11.8 (2009): 1052-64.
36. Lee SY, Nakagawa T, Reddi AH. "Mesenchymal progenitor cells derived from synovium and infrapatellar fat pad as a source for superficial zone cartilage tissue engineering: analysis of superficial zone protein/lubricin expression". *Tissue Engineering Part A* 16.1 (2010): 317-25.
37. Dragoo JL, Samii B, Zhu M, Hame SL, Thomas BJ, Lieberman JR, Hedrick MH, Benhaim P. "Tissue-engineered cartilage and bone using stem cells from human infrapatellar fat pads". *Journal of Bone and Joint Surgery, British Volume* 85.5 (2003): 740-7.
38. Zimmerlin L, Donnenberg VS, Pfeifer ME, Meyer EM, Pàult B, Rubin JP, Donnenberg AD. "Stromal vascular progenitors in adult human adipose tissue". *Cytometry* 77.1 (2010): 22-30.

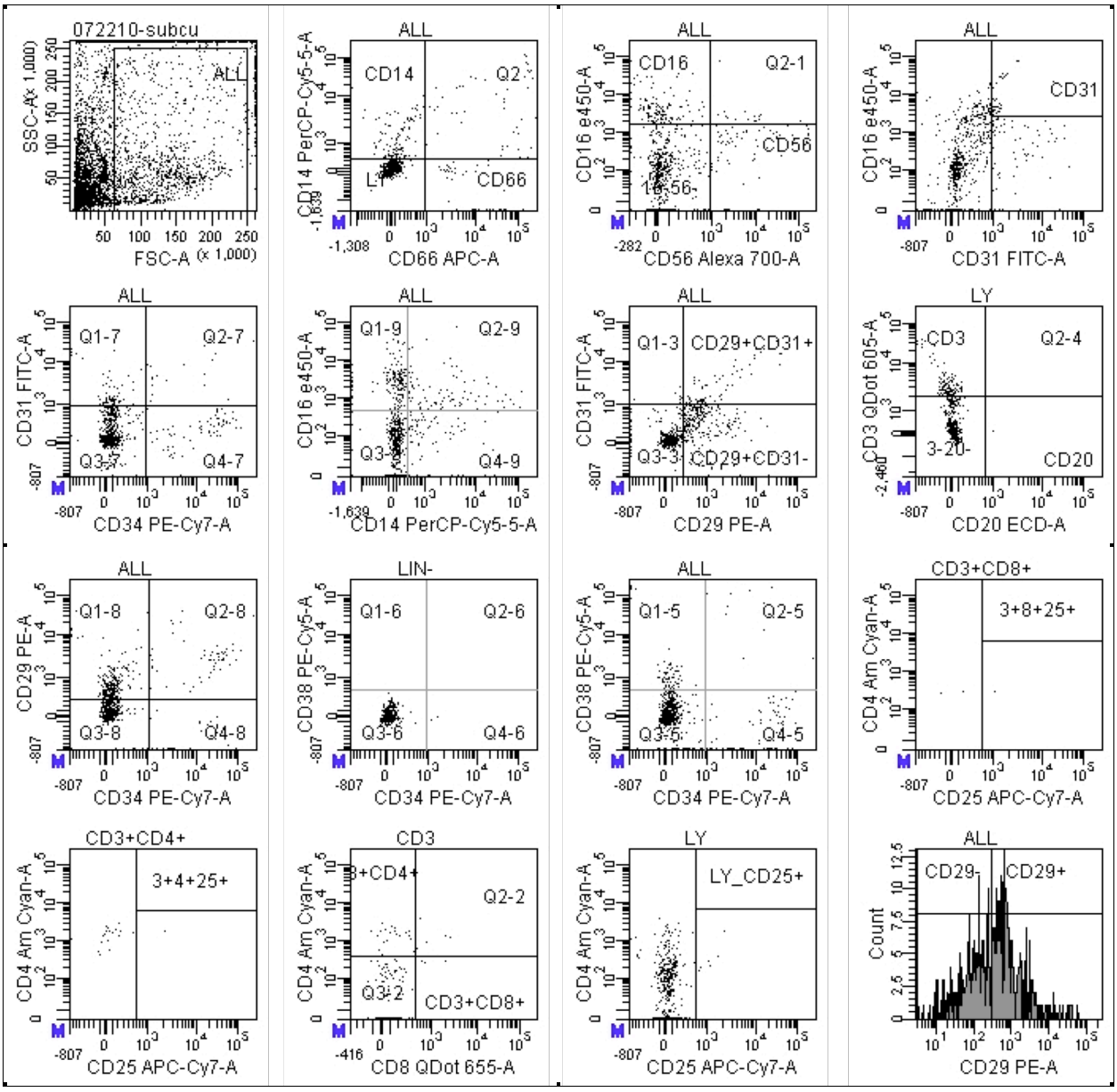

Figure S-2: Donor 5 Subcutaneous Adipose Tissue FACS Analysis

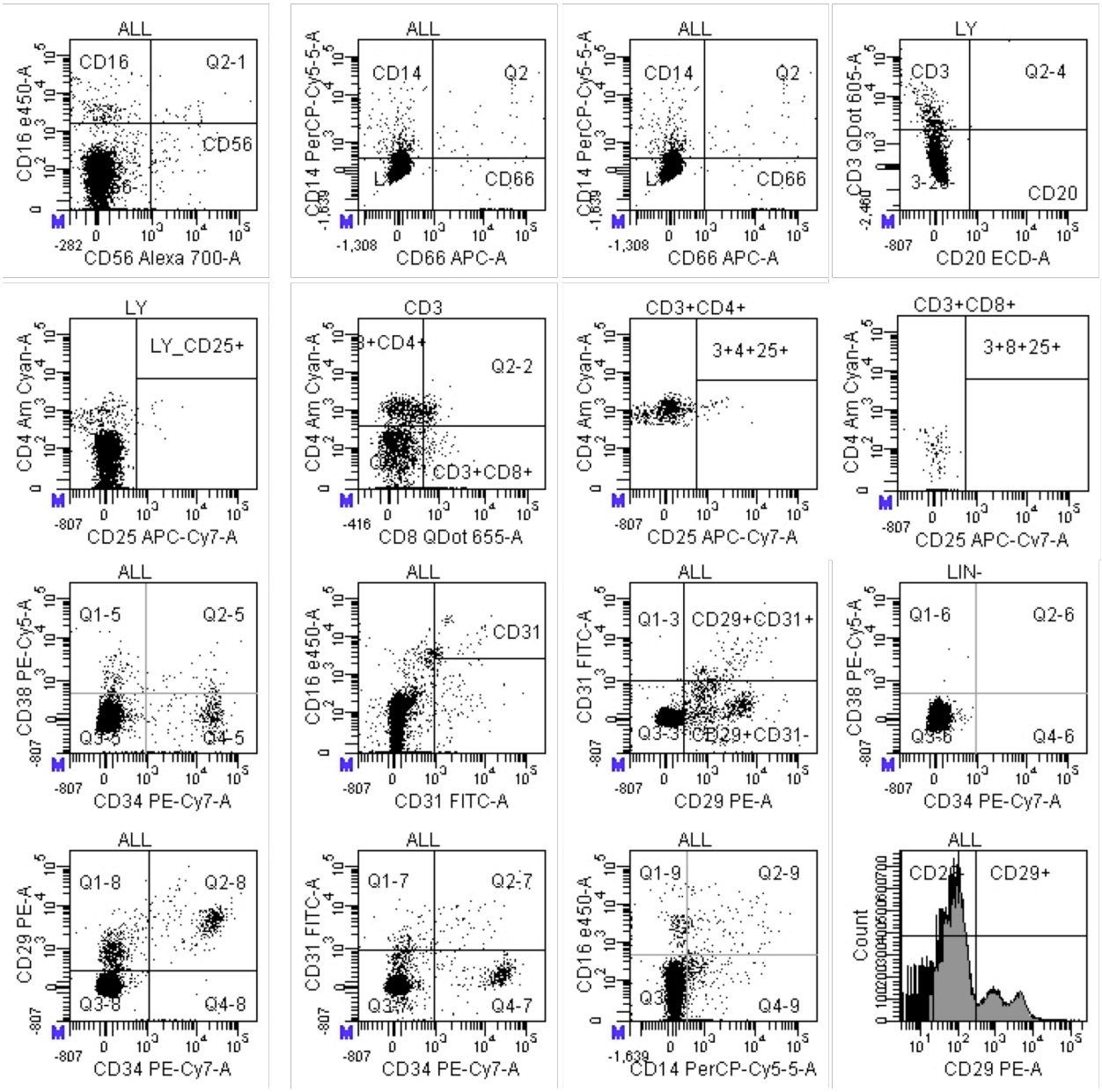

Figure S-2: Donor 5 Infrapatellar Fat Pad FACS Analysis